



Published in final edited form as:

Nat Commun. 2013 ; 4: 2150. doi:10.1038/ncomms3150.

Large fiber size in skeletal muscle is metabolically advantageous

Ana Gabriela Jimenez^{1,a}, Richard M. Dillaman¹, and Stephen T. Kinsey^{1,*}

¹Department of Biology and Marine Biology, University of North Carolina Wilmington, Wilmington, North Carolina, 601 South College Rd, Wilmington, NC 28403

Abstract

Skeletal muscle fiber size is highly variable, and while diffusion appears to limit maximal fiber size, there is no paradigm for the control of minimal size. The optimal fiber size hypothesis posits that the reduced surface area to volume (SA:V) in larger fibers reduces the metabolic cost of maintaining the membrane potential, and so fibers attain an optimal size that minimizes metabolic cost while avoiding diffusion limitation. Here we examine changes during hypertrophic fiber growth in metabolic cost and activity of the Na⁺-K⁺-ATPase in white skeletal muscle from crustaceans and fishes. We provide evidence for a major tenet of the optimal fiber size hypothesis by demonstrating that larger fibers are metabolically cheaper to maintain, and the cost of maintaining the membrane potential is proportional to fiber SA:V. The influence of SA:V on metabolic cost is apparent during growth in 16 species spanning a 20-fold range in fiber size, suggesting that this principle may apply widely.

INTRODUCTION

While it is generally accepted that cell size is regulated, the mechanisms that govern cell size are poorly understood¹⁻³. Skeletal muscle fibers are multi-nucleated syncytia that are among the largest cell types, and across the animal kingdom range in diameter from several microns to thousands of microns. The maximal fiber size seems to be limited by diffusion constraints associated with aerobic metabolism, which relies on the transport of O₂ from the blood to the mitochondria and subsequent diffusion of ATP from mitochondria to cellular ATPases³⁻⁵. In contrast, there is no paradigm to explain the limitations on minimal fiber size. This is a substantial gap in understanding, since many skeletal muscle fiber types attain sizes that make them nearly diffusion limited, suggesting that they may be under selective

Users may view, print, copy, download and text and data- mine the content in such documents, for the purposes of academic research, subject always to the full Conditions of use: http://www.nature.com/authors/editorial_policies/license.html#terms

*Corresponding author kinseys@uncw.edu.

^aCurrent address: Department of Evolution, Ecology and Organismal Biology, The Ohio State University, 318 W. 12th Ave. Columbus, OH 43204.

AUTHOR CONTRIBUTIONS

AGJ collected specimens, performed microscopic, NMR and fluorometric assays, and wrote a draft of the manuscript. RMD performed microscopic training, supervised the microscopy, and edited the manuscript. STK supervised the project, developed the NMR approach, provided technical training, conducted data analyses, and revised the manuscript.

COMPETING FINANCIAL INTERESTS

The authors declare no competing financial interests.

pressure to be as large as possible^{4,5}. For instance, some skeletal muscle fibers undergo structural changes during hypertrophic increases in fiber size, such as mitochondrial and nuclear redistribution or shifts in growth patterns⁴⁻⁹, and reaction-diffusion models have demonstrated that these changes are necessary to offset the increasing diffusion constraints associated with fiber growth^{6-7, 10-12}. Thus, there are structural and metabolic responses that allow fibers to grow larger than would otherwise be possible while still retaining full function.

In an effort to explain the very large fibers found in white muscle of some cold-water fishes, Johnston et al.¹³⁻¹⁵ proposed the 'optimal fiber size hypothesis', which states that fiber size represents a balance between the need for small fibers that promote rapid diffusive flux and potential metabolic cost savings associated with large fibers that have a low surface area:volume (SA:V) over which to maintain the membrane potential. Muscle represents a large fraction of body mass in many animals, and in humans accounts for 20-30% of total resting O₂ consumption¹⁶. A major source of ATP demand in muscle is maintenance of the membrane potential by the Na⁺-K⁺-ATPase¹⁷, and this is the only sizable ATP sink in resting muscle that is associated with the sarcolemmal membrane and therefore potentially sensitive to fiber SA:V. We previously found that in lobster abdominal muscle that undergoes hypertrophic fiber growth, the smaller fibers of juvenile animals had a 2-fold higher SA:V than the much larger fibers of adults, and this was associated with a 2-fold higher ATP cost of the Na⁺-K⁺-ATPase (in resting muscle preparations) and a 2-fold higher maximal enzyme activity of the Na⁺-K⁺-ATPase (in muscle homogenates)¹⁸. These results suggested that the very large fibers found in this species are advantageous because of a reduced SA:V, as proposed by Johnston et al.¹³⁻¹⁵. However it remains unclear whether this is a general principle that applies over a broad fiber size range.

The present study tested whether larger fibers are cheaper to maintain by evaluating the fiber SA:V-dependence of Na⁺-K⁺-ATPase cost and maximal activity in white muscle from small and large size classes of 16 species of crustaceans and fishes. White muscle from these groups was selected because it typically grows hypertrophically in crustaceans^{4, 8, 19} and fishes^{5, 20, 21}, constitutes a large fraction of body mass, and is used relatively infrequently for burst contraction. Therefore, economy of maintenance of resting muscle may be under particularly strong positive selection in these groups. Further, in some species hypertrophic growth is coupled to a very large increase in post-metamorphic body mass, leading to dramatic increases in fiber size during animal growth. By examining changes in Na⁺-K⁺-ATPase cost and activity during growth within species, we were able to account for variation linked to phylogeny. The 16 species selected had a large range in mean body mass and mean fiber size both within and between species, and included a phylogenetically diverse group of marine and freshwater animals, allowing us to test the hypothesis that large fibers are cheaper to maintain. The absolute and fractional ATP cost in resting muscle, and the maximal enzyme activity of the Na⁺-K⁺-ATPase in muscle homogenates were proportional to changes in SA:V, providing the first experimental evidence across a wide range of fiber sizes and species that large fiber size is likely metabolically advantageous. This may explain why many fibers grow to sizes that put them on the brink of diffusion limitation.

RESULTS

Body mass and fiber size

The species examined, body masses and fiber sizes for each size class are shown in Table 1. In each species, there was no overlap in the body mass range of the small and large size classes, but there was some overlap in fiber diameter range between size classes primarily due to the presence of some small fibers in each large size class. Across species, the mean body mass ranged from <0.1 g to 687 g (a nearly 7000-fold range) and mean fiber size ranged from 38 μm to 763 μm (a 20-fold range). Since SA:V of a cylinder (excluding the ends) is $2/\text{radius}$, this corresponds to a 20-fold range in fiber SA:V. For both body mass and fiber size there was a significant effect of species ($p < 0.0001$ for both, Kruskal-Wallis tests) and size class when all species were pooled ($p < 0.0001$ for both, Wilcoxon tests). Pairwise comparisons indicated that body mass and white muscle fiber diameter from every species was significantly greater in the large size class than in the small size class (Wilcoxon tests with significance level adjusted for multiple comparisons; see Methods), indicative of hypertrophic fiber growth (Table 1).

ATP cost and maximal activity of the $\text{Na}^+\text{-K}^+\text{-ATPase}$

To calculate the ATP cost of the $\text{Na}^+\text{-K}^+\text{-ATPase}$ in resting muscle, the rate of depletion of phosphocreatine (PCr; fishes) or arginine phosphate (AP; crustaceans) was measured in small muscle preparations using ^{31}P -nuclear magnetic resonance (NMR). ^{31}P -NMR spectra were collected while energy metabolism was inhibited with cyanide (CN) and iodoacetate (IA), and the rate of PCr or AP depletion was used to determine the total ATP demand in the resting muscle. Here, the rate of PCr or AP consumption is equivalent to the rate of resting ATP demand. These experiments were repeated under identical conditions (CN and IA were again used to inhibit energy metabolism), except that ouabain (OU) was also added to inhibit the $\text{Na}^+\text{-K}^+\text{-ATPase}$. The reduction in the PCr or AP depletion rate when OU was added was used to calculate the absolute $\text{Na}^+\text{-K}^+\text{-ATPase}$ energetic cost (mM of ATP hydrolyzed per min) as well as the fraction of total ATP consumption attributable to the $\text{Na}^+\text{-K}^+\text{-ATPase}$ in isolated resting muscle (see Methods). In separate experiments, the maximal enzyme activity of the $\text{Na}^+\text{-K}^+\text{-ATPase}$ was measured in muscle homogenates to determine whether the total capacity for Na^+ and K^+ transport was also dependent on fiber SA:V (see Methods).

The small muscle preparations displayed good metabolic stability during NMR experiments, based on high initial PCr or AP to ATP ratios, and low inorganic phosphate (P_i) in the spectra from all species (Fig. 1a). In some representative species (*P. argus*, *H. americanus*, *C. sapidus* and *C. striata*), additional experiments were run where tissues were maintained in oxygenated saline to ensure that there was no change in PCr or AP concentration over the 30 min time course of the NMR experiments. In contrast, addition of inhibitors of oxidative phosphorylation (CN) and glycolysis (IA) produced linear reductions in PCr or AP over time (and corresponding increases in P_i), and when OU was simultaneously added the rate of PCr or AP depletion was reduced (Fig. 1b), allowing us to determine the absolute and fractional cost of the $\text{Na}^+\text{-K}^+\text{-ATPase}$ in resting muscle from the difference in the slopes.

Table 2 presents the PCr and AP mean depletion rates and calculated absolute and fractional costs of the Na⁺-K⁺-ATPase in resting muscle, along with the Na⁺-K⁺-ATPase maximal activity in muscle homogenates. Kruskal-Wallis analyses revealed effects of species on PCr and AP depletion rate in both size classes (small: p=0.0084; large: p<0.0001), and Wilcoxon tests found significant differences between inhibitor treatments in both size classes (small: p<0.0001; large: p<0.0001). The species effect is largely related to the much higher depletion rates in crustaceans than in fishes. The difference between treatments reflects the fact that the mean depletion rate was lower when OU was added in every species and size class, as expected, although pairwise comparisons within species were not significant following adjustment of the significance level for multiple tests. The absolute and fractional Na⁺-K⁺-ATPase cost is derived from differences in the mean depletion rates, and therefore has no error, but in 13 of 16 species (absolute) and 14 of 16 species (fractional) the Na⁺-K⁺-ATPase cost was lower in the large size class. When these data were pooled across species, the absolute cost (p=0.035) and fractional cost (p=0.019) were significantly lower in the large size class as expected (Wilcoxon tests). The Na⁺-K⁺-ATPase activity in muscle homogenates had a similar pattern, where a significant effect of species was found (p<0.0001; Kruskal-Wallis test), and there was a significant difference between size classes when all of the species were pooled (p<0.0001; Wilcoxon test). In every species, the large size class had lower activity, which accounts for the size class difference, although pairwise comparisons revealed that most of these differences within a species were not significant following adjustment of the significance level for multiple tests (Wilcoxon tests, Table 2).

Na⁺-K⁺-ATPase cost and activity are dependent on SA:V

Supplementary Figure S1 shows the mean fiber sizes and mean fractional cost and activity measurements for the small and large size class of each species fitted to a SA:V curve (data from Tables 1 and 2). As hypothesized, the changes in Na⁺-K⁺-ATPase fractional cost in resting muscle (Supplementary Fig. S1a) and activity in homogenates (Supplementary Fig. S1b) during hypertrophic fiber growth were proportional to changes in SA:V. The same pattern exists for absolute Na⁺-K⁺-ATPase cost, and when these data were normalized to show all species on a single plot, it is clear that the absolute ATP cost (Fig. 2a) and enzyme activity (Fig. 2b) demonstrate SA:V dependence over a broad fiber size range. There clearly is some deviation from the SA:V dependence, which likely arises from experimental and biological variation. However, the fact that fundamentally different types of measurements of fractional/absolute cost (Fig. 2a and Supplementary Fig. S1a) in intact resting muscle and maximal activity in homogenates (Fig. 2b and Supplementary Fig. S1b) yield the same pattern provides strong support for our methodology and conclusions that larger fibers are cheaper to maintain.

DISCUSSION

The present study provides experimental evidence in a broad range of species and fiber sizes that large fibers are metabolically advantageous because they are cheaper to maintain. The reduced maintenance costs of larger fibers may also explain prior findings that indicate that many fibers are on the brink of diffusion limitation in adult animals (reviewed in 5). During hypertrophic fiber growth in white muscle of fishes and crustaceans, there is a dramatic shift

in the distribution of mitochondria from the fiber interior to the periphery, which limits O₂ diffusion distances and enhances aerobic metabolic rates, and an opposing shift in nuclei from the fiber periphery to the interior, which limits macromolecular diffusion distances within the myonuclear domain and enhances rates of protein turnover^{4–12}. Thus, these organelle distribution shifts during fiber growth allow the fibers to grow larger than would otherwise be possible. Modeling indicated that aerobic metabolism is the most important limiter of fiber size, and that if fibers were to continue to grow hypertrophically beyond the maximal size found in adults, aerobic metabolism would become substantially diffusion limited. In fact, in white muscle from black sea bass (*Centropristis striata*), as the animal grows to near maximal body size and our models predict that further fiber growth would result in diffusion limitation, the muscle fibers shift from exclusively hypertrophic growth to largely hyperplastic growth and/or fiber splitting⁹. These and other prior results, when coupled with the findings of the present study, are consistent with the optimal fiber size hypothesis, where fibers reach a maximal size that minimizes maintenance cost without becoming constrained by diffusion.

Johnston et al.^{13–15} originally proposed the optimal fiber size hypothesis to explain the presence of very large white fibers in some cold water fishes, but the influence of fiber size on SA:V is actually greatest in small fibers. Fibers with a maximal diameter less than about 100 μm had a large decrease in both cost and activity during hypertrophic growth, while the absolute cost savings associated with continued growth to hundreds of microns is smaller (Fig. 2). Thus, the metabolic advantages of hypertrophic fiber growth are likely greatest in animals with relatively small fibers, including mammals and birds, where the typical increase in fiber size during animal growth would lead to a large change in SA:V. Further, most muscles grow by a combination of hyperplasia and hypertrophy, and the linkage between muscle growth pattern and metabolic rate suggests that the activation of hyperplastic growth that produces small fibers would also lead to an elevation of muscle, and likely whole animal, resting metabolic rate.

The present study provides evidence for a key component of the optimal fiber size hypothesis, but does not demonstrate that maximizing fiber size is under positive selective pressure as proposed previously^{13–15}. However, prior work has shown that diversity in body size attained following post-glacial invasions of freshwater habitats by fishes was associated with parallel changes in muscle growth patterns in a manner consistent with a shift toward a more optimal fiber size²². In Arctic charr and threespine stickleback selection for dwarfism is associated with a dramatic reduction in the maximal number of fibers in muscle (by as much as 85% in Arctic charr). That is, as the maximal adult body mass is reduced fewer fibers are needed to meet the demands for muscle growth. This leads to an adult fiber diameter that is greatly increased in the dwarf populations over what it would have been had there not been a reduction in new fiber formation. In Arctic charr, the adaptive increase in adult fiber size of the dwarf population reduced the SA:V by up to 35%, which would be expected to reduce the cost of maintaining ionic gradients across the sarcolemma by a similar amount. In a rapidly evolving population of dwarf sticklebacks, adaptation of new fiber recruitment patterns occurred within ~10 generations, suggesting that there is intense selection for optimal fiber size in this population²². Similarly, the very large fiber size

among many members of the notothenioid lineage of fishes appears to be a mechanism to reduce energy demand and is associated with adaptation to the cold water of the Southern Ocean. In this case, the very low metabolic demands of the muscle tissues relax diffusion constraints, allowing the fibers to grow to extreme dimensions¹³.

While the data were normalized in Fig. 2 so that all species could be plotted on a single SA:V curve, there was a strong phylogenetic signature in all of the results (Table 2). This was most obvious when comparing the two major groups of animals, where Na⁺-K⁺-ATPase absolute cost, fractional cost, and activity, as well as the total ATP demand in resting muscle (the IA + CN treatments in Table 2), were higher in muscle from crustaceans than fishes (Wilcoxon tests, $p < 0.0006$ for all). For example, in crustaceans the Na⁺-K⁺-ATPase cost accounted for an average of $57 \pm 3\%$ of the total energy expenditure in resting muscle from the small size classes of animals, and $45 \pm 4\%$ of total energy expenditure in the large size classes. In fishes the Na⁺-K⁺-ATPase accounted for $35 \pm 4\%$ of the total ATP demand in resting muscle from animals in the small size classes, but only $15 \pm 3\%$ in the large size classes. The greater effect of hypertrophic growth on ATP cost seen in the fishes compared to crustaceans reflects the fact that the fish species examined generally had smaller fibers than the crustaceans, so small increases in fiber size led to large changes in SA:V. The fractional costs of the Na⁺-K⁺-ATPase measured in the present study were consistent with previous results from studies in skeletal muscle from sheep²³, calves²³, mice²⁴, rats²⁵, and lugworms²⁶. Thus, the Na⁺-K⁺-ATPase cost represented a sizable fraction of the total resting ATP demand, indicating that reducing fiber SA:V can lead to a substantial energetic saving. The phylogenetic dependence of the data illustrate the importance of examining the *change* in cost and activity associated with fiber growth within each species, as the SA:V dependence is otherwise not apparent.

While there was considerable variation among species the absolute Na⁺-K⁺-ATPase cost was linearly dependent on the maximal activity across all species and size classes (cost = $0.0028 \times \text{activity} + 0.025$, $r^2 = 0.25$, $p = 0.0038$; data in Table 2). This is consistent with the linear dependence of skeletal muscle oxygen consumption on Na⁺-K⁺-ATPase activity in rat²⁵. The implication of this finding is that the number of Na⁺-K⁺-ATPase pumps largely dictates cost, and within a species pump density does not change during growth and total pump number parallels total sarcolemmal surface area (Fig. 2 and Supplementary Fig. S1). Therefore, reducing the expression of the Na⁺-K⁺-ATPase does not appear to be a strategy to reduce costs in the smaller fibers of the small size class animals.

In summary, this study provides the first direct evidence over a broad range of species and fiber sizes that large fibers are advantageous because they are cheaper to maintain. These results, coupled with prior work indicating that large fiber size is under positive selection and that fibers often attain a maximal size that is on the brink of diffusion limitation, are consistent with the optimal fiber size hypothesis proposed by Johnston et al.¹³⁻¹⁵. The present study also suggests that there is a link between fiber size and whole animal metabolic rate.

METHODS

Animal collection and fiber diameter measurements

Small and large size classes of fishes and crustaceans were collected locally or supplied by vendors. Fiber diameter and body mass of each species and size class were measured according to previous protocols from Hardy et al.⁷ and Jimenez et al.^{10, 18}. All procedures were approved by the University of North Carolina Wilmington Institutional Animal Care and Use Committee.

Total ATP demand and Na⁺-K⁺-ATPase cost in resting muscle

The total resting ATP demand and the demand of the Na⁺-K⁺-ATPase were determined in small isolated preparations, ~1 mm in diameter, of anterior epaxial muscle in fishes⁶, abdominal extensor muscle in shrimp, lobsters and crayfish^{10,18} and fifth periopod light levator muscle from crabs⁷⁻⁸. The muscle preparations were secured at resting length to the outside of a section of rigid superfusion tubing (1 mm O.D.) and saline flow was provided by peristaltic pumps. The rigid section of tubing with the muscles attached was inserted into a 5 mm NMR tube so that flow through the superfusion tubing entered at the bottom of the NMR tube and exited via a separate superfusion tube at the top, thus washing over the muscle preparation¹⁸.

The rate of decrease of PCr or AP was monitored over time with ³¹P-NMR in the presence of metabolic inhibitors¹⁸. PCr and AP are substrates in the creatine kinase (CK) and arginine kinase (AK) reactions, respectively, which catalyze the transfer of a phosphoryl group from PCr or AP to ADP, forming ATP. CK and AK have high activity that far exceeds the ATP turnover rate in resting white muscle, so the substrates and products of the reactions are maintained at equilibrium, and there is a 1:1 stoichiometry of PCr hydrolyzed to ATP formed. Therefore, if ATP supply is inhibited, PCr or AP concentration will decrease as ATP is consumed by cellular processes such as the Na⁺-K⁺-ATPase. In the present case, the total resting ATP demand was determined from the rate of PCr or AP decrease while energy metabolism was inhibited with 2.5 mM CN to block oxidative phosphorylation and 1 mM IA to block glycolysis in the appropriate saline solution²⁷⁻³⁰. The ATP cost of the Na⁺-K⁺-ATPase was determined from the reduction in the rate of PCr or AP depletion when energy metabolism was blocked as above, while simultaneously treating the muscle with 5 mM OU, which inhibits the Na⁺-K⁺-ATPase (Fig. 1). A total of 339 NMR rate measurements were performed, where NMR spectra were collected every 3 min on a Bruker 400 or 600 MHz DMX spectrometer to determine relative concentrations of PCr or AP, ATP and inorganic phosphate (P_i). Peak areas were converted to concentration by assuming a total high-energy phosphate concentration of 50 mM. Linear regression was used to measure the rate of PCr or AP depletion.

Na⁺-K⁺-ATPase maximal activity in muscle homogenates

A K⁺-stimulated 3-*O*-methylfluorescein phosphatase (MFPase) assay was used to measure Na⁺-K⁺-ATPase maximal activity in muscle homogenates as described previously^{10, 31-33}. Activity was determined using spectrofluorometry at an excitation wavelength of 475 nm and an emission wavelength of 515 nm (Promega Luminometer 20/20 with a Glomax blue

module; Madison, WI, USA), on small tissue sample homogenates from each size class and species. The addition of $160 \mu\text{mol l}^{-1}$ 3-*O* methylfluorescein phosphate led to a linear increase in fluorescence, which was recorded and followed by addition of $10 \mu\text{mol l}^{-1}$ KCl to activate the $\text{Na}^+\text{-K}^+\text{-ATPase}$. K^+ -dependent 3-*O*-MFPase activity (i.e., $\text{Na}^+\text{-K}^+\text{-ATPase}$ activity) was determined by subtracting activity before the addition of KCl from activity after the addition of KCl.

Statistical analyses

Data were non-normally distributed and could not be transformed to meet this assumption so all analyses were conducted using non-parametric tests. For body mass, fiber size, and $\text{Na}^+\text{-K}^+\text{-ATPase}$ activity, Kruskal-Wallis analyses were used to test for effects of species, and Wilcoxon tests were used to compare size classes when all species were pooled (overall size effect), as well as for pairwise comparisons between size classes within each species. In the latter comparisons, we adjusted the significance level to account for multiple tests of the same hypothesis following the procedures of Hochberg³⁴. To evaluate the PCr and AP depletion rate data, Kruskal-Wallis tests were used to test for significant effects of species within each size class, and Wilcoxon tests were used to test for differences between treatments (CN+IA or CN+IA+OU) within each size class when all species were pooled. Pairwise comparisons were made to test for differences between treatments (CN+IA or CN+IA+OU) within each species and size class using Wilcoxon tests, again adjusting for multiple tests. The $\text{Na}^+\text{-K}^+\text{-ATPase}$ absolute cost and fractional cost were derived from mean PCr or AP depletion rates and therefore had no error term, preventing a comparison of size classes within species. However, Wilcoxon tests were used to compare the size classes when the absolute and fractional cost data were pooled across species. Results were considered significant if $p < 0.05$, except in cases where significance levels were adjusted as described above³⁴.

Supplementary Material

Refer to Web version on PubMed Central for supplementary material.

ACKNOWLEDGMENTS

The authors would like to thank Captain Jeff Wolfe, Jay Styron, Ken Johns, Gerry Compeau, Jeremy Burnett, Leigh Anne Harden, Kenneth Kelly, Carolina Priester, Trent Ross, Jeff Harms, Daniel Russo, Robert Trost, Ginger Winder, Jessica Snoddy, Dr. T. Lankford, Ed Arb, Ellie Kinsey, and Nathan Kinsey for their help collecting the animals used in this study. We would also like to thank Robbie McNeill for his contribution in collecting the $\text{Na}^+\text{-K}^+\text{-ATPase}$ activity data and Mark Gay for help with microscopy. This research was supported by NSF (IOS-0719123) and NIH (NIAMS R15-AR052708) grants to STK and Sigma Xi and SICB grants-in-aid of research grants to AGJ.

REFERENCES

1. Stocker H, Grafen E. Genetic control of cell size. *Curr. Op. Gen. Dev.* 2000; 10:529–535.
2. Guertin, DA.; Sabatini, DM. eLS. Chichester: John Wiley & Sons Ltd; 2006. Cell Size Control. <http://www.els.net>
3. Van Wessel T, de Haan A, van der Laarse WJ, Jaspers RT. The muscle fiber type-fiber size paradox: hypertrophy or oxidative metabolism. *Eur. J. Appl. Physiol.* 2010; 110:665–694. [PubMed: 20602111]

4. Kinsey ST, Hardy KM, Locke BR. The long and winding road: influences of intracellular metabolite diffusion on cellular organization and metabolism in skeletal muscle. *J. Exp. Biol.* 2007; 210:3505–3512. [PubMed: 17921152]
5. Kinsey ST, Locke BR, Dillaman RM. Molecules in Motion: Influences of diffusion on metabolic structure and function in skeletal muscle. *J. Exp. Biol.* 2011; 214:263–274. [PubMed: 21177946]
6. Nyack AC, Locke BR, Valencia A, Dillaman RM, Kinsey ST. Scaling of post-contractile phosphocreatine recovery in fish white muscle: effect of intracellular diffusion. *Am. J. Physiol.* 2007; 292:R1–R12.
7. Hardy KM, Dillaman RM, Locke BR, Kinsey ST. A skeletal muscle model of extreme hypertrophic growth reveals the influence of diffusion on cellular design. *Am. J. Physiol.* 2009; 296:R1855–R1867.
8. Hardy KM, Lema SC, Kinsey ST. The metabolic demands of swimming behavior influence the evolution of skeletal muscle fiber design in the brachyuran crab family Portunidae. *Mar. Biol.* 2010; 157:221–236.
9. Priester C, Morton LC, Kinsey ST, Watanabe WO, Dillaman RM. Growth patterns and nuclear distribution in white muscle fibers from black sea bass *Centropristis striata* (Linnaeus): evidence for the influence of diffusion. *J. Exp. Biol.* 2011; 214:1230–1239. [PubMed: 21430198]
10. Jimenez AGJ, Locke BR, Kinsey ST. The influence of oxygen and high-energy phosphate diffusion on metabolic scaling in three species of tail-flipping crustaceans. *J. Exp. Biol.* 2008; 211:3214–3225. [PubMed: 18840655]
11. Locke BR, Kinsey ST. Diffusional constraints on energy metabolism in skeletal muscle. *J. Theor. Biol.* 2008; 254:417–429. [PubMed: 18619978]
12. Pathi B, Kinsey ST, Locke BR. The formation and functional consequences of heterogeneous mitochondrial distributions in skeletal muscle. *J. Exp. Biol.* 2012; 215:1871–1883. [PubMed: 22573766]
13. Johnston IA, et al. Reduction in muscle fibre number during the adaptive radiation of Notothenioid fishes: a phylogenetic perspective. *J. Exp. Biol.* 2003; 206:2595–2609. [PubMed: 12819266]
14. Johnston IA, et al. Rapid evolution of muscle fibre number in post-glacial populations of charr *Salvelinus alpinus*. *J. Exp. Biol.* 2004; 207:4343–4360. [PubMed: 15557021]
15. Johnston IA, Abercromby M, Andersen O. Muscle fibre varies with haemoglobin phenotype on Atlantic cod as predicted by the optimal fibre number hypothesis. *Biol. Lett.* 2006; 2:590–592. [PubMed: 17148296]
16. Zurlo F, Larson K, Bogardus C, Ravussin E. Skeletal muscle metabolism is a major determinant of resting energy expenditure. *J. Clin. Invest.* 1990; 86:1423–1427. [PubMed: 2243122]
17. Milligan LP, McBride BW. Energy costs of ion pumping by animal tissues. *J. Nutr.* 1985; 115:1374–1382. [PubMed: 2413191]
18. Jimenez AGJ, Dasika SK, Locke BR, Kinsey ST. An evaluation of muscle maintenance costs during fiber hypertrophy in the lobster *Homarus americanus*: Are larger muscle fibers cheaper to maintain? *J. Exp. Biol.* 2011; 214:3688–3697. [PubMed: 21993799]
19. Bittner GD, Traut DL. Growth of Crustacean muscles and muscle fibers. *J. comp. Physiol.* 1978; 124:277–285.
20. Weatherley, A.; Gill, H. *Biology of Fish Growth*. San Diego, CA: Academic press; 1987.
21. Valente LMP. Growth dynamics of white and red muscle fibers in fast- and slow- growing strains of rainbow trout. *J. fish biol.* 1999; 55:675–691.
22. Johnston IA, et al. Universal scaling rules predict evolutionary patterns of myogenesis in species with indeterminate growth. *Proc. R. Soc. B.* 2012; 279:2255–2261.
23. Gregg VA, Milligan LP. *In vitro* energy costs of Na⁺-K⁺-ATPase activity and protein synthesis in muscle from calves differing in age and breed. *Br. J. Nutr.* 1982; 48:65–71. [PubMed: 6285953]
24. Gregg VA, Milligan LP. Inhibition by ouabain of the O₂ consumption of the mouse (*Mus musculus*) soleus and diaphragm muscles. *Gen Pharmac.* 1980; 11:323–325.
25. Asano Y, Liberman UA, Eldelman IS. Relationships between Na⁺-dependent respiration and Na⁺K⁺-adenosine triphosphatase activity in rat skeletal muscle. *J. Clin. Invest.* 1976; 57:368–376. [PubMed: 130385]

26. Pörtner HO, Bock C, Reipschlag A. Modulation of the cost of pH_i regulation during metabolic depression: A 31P-NMR study in invertebrate (*Sipunculus nudus*) isolated muscle. *J. Exp. Biol.* 2000; 203:2417–2428. [PubMed: 10903156]
27. van Harrevelde A. Physiological saline for crayfish. *Proc. Soc. Exp. Biol. Med.* 1936; 34:428.
28. Cole WH. A perfusing solution for the lobster (*Homarus*) heart and the effect of its constituent ions on the heart. *J. Cell Biol.* 1941; 25:1–6.
29. Hoar, WS.; Hickman, CP. *A Laboratory Companion for General and Comparative Physiology*. 3rd edn. Vol. 307. New Jersey: Prentice-Hall; 1983.
30. Hoffman EK, Hoffman E, Lang F, Zadunaisky JA. Control of Cl^- transport in the operculum of *Fundulus heteroclitus*: long- and short-term salinity adaptation. *Biochim. Biophys Acta.* 2002; 1566:129–139. [PubMed: 12421544]
31. Sandiford SDE, Green HJ, Ouyang J. Mechanisms underlying increases in rat soleus $\text{Na}^+\text{-K}^+$ -ATPase activity by induced contractions. *J. Appl. Physiol.* 2005; 99:2222–2232. [PubMed: 16109830]
32. Fraser SF, McKenna MJ. Measurement of $\text{Na}^+\text{-K}^+$ -ATPase activity in human skeletal muscle. *Anal. Biochem.* 1998; 258:63–67. [PubMed: 9527849]
33. Barr DJ, Green HJ, Lounsbury DS, Rush JWE, Ouyang J. $\text{Na}^+\text{-K}^+$ -ATPase properties in rat heart and skeletal muscle 3 mo after coronary artery ligation. *J. Appl. Physiol.* 2005; 99:656–664. [PubMed: 15817721]
34. Hochberg Y. A sharper Bonferonni procedure for multiple tests of significance. *Biometrika.* 1988; 75(4):800–802.

a Cyanide + iodoacetate Cyanide + iodoacetate + ouabain

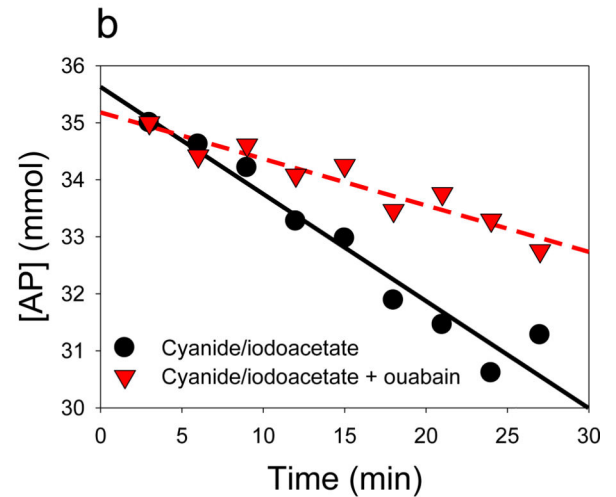
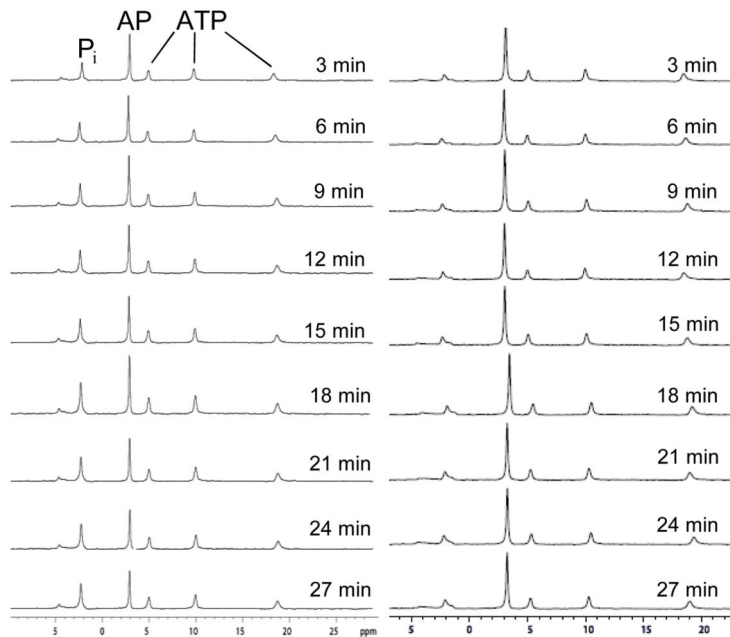


Figure 1.

Example of ³¹P-NMR measurement of AP depletion rates. Representative experiment showing changes over time in (a) NMR spectra and (b) AP concentration during treatment with CN and IA or CN, IA and OU. The AP depletion rate was higher when energy metabolism alone was blocked with CN and IA than when energy metabolism and the Na⁺-K⁺-ATPase were inhibited with CN, IA and OU. The CN and IA treatment yields the total ATP demand, and the difference between slopes is the ATP cost of the Na⁺-K⁺-ATPase in isolated resting muscle.

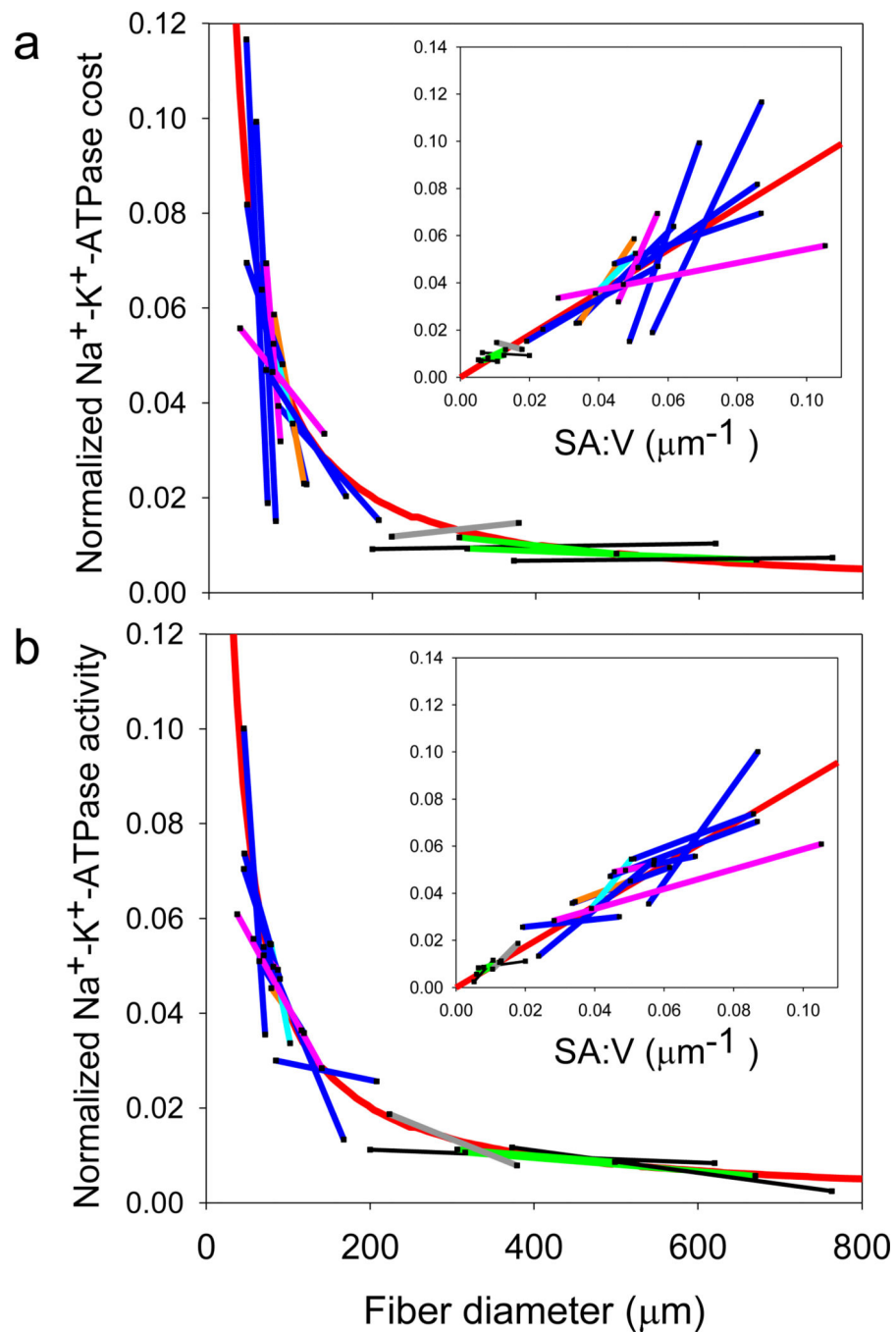


Figure 2. $\text{Na}^+\text{-K}^+$ ATPase cost and enzymatic activity during hypertrophic fiber growth. (a) Absolute $\text{Na}^+\text{-K}^+$ ATPase cost and (b) maximal enzymatic activity, normalized to fit all species on a single plot. The straight colored lines connect the mean values for the small and large size classes (for visualization purposes only) and show that the changes in cost and activity during hypertrophic growth follow the pattern predicted for SA:V (red line) over a wide fiber size range. The data were normalized by dividing the absolute cost of the $\text{Na}^+\text{-K}^+$ ATPase (Table 2) by the adjustable coefficient, α , the value of which was determined for

each species from an iterative curve fit as described in Supplemental Figure S1, allowing all data to be plotted in a single graph. The line color represents species group (pink = marine shrimp, green = marine lobster, gray = freshwater crayfish, black = marine crab, blue = marine teleost fish, cyan = freshwater teleost fish, and orange = marine elasmobranch). The insets are the same data plotted as a linear function of SA:V (linear regression equations: normalized cost = $0.942(\text{SA:V}) + 0.002$, $r^2=0.72$, $p<.0001$ (t-test, $n=32$); normalized activity = $0.812(\text{SA:V}) + 0.003$, $r^2=0.86$, $p<0001$ (t-test, $n=32$)).

Table 1

Species and size class information.

Species	Type of animal	Common name	Body mass (g)		Fiber diameter (µm)	
			Small [†] §	Large [†] §	Small [†] §	Large [†] §
<i>Farfantepenaeus aztecus</i>	Marine shrimp	Brown shrimp	1.6 ± 0.05 (10)	10.8 ± 0.2 (13)*	37.9 ± 0.9 (5)	141.3 ± 3.7 (6)*
<i>Palaemonetes pugio</i>	Marine shrimp	Ghost shrimp	0.1 ± 0.001 (10)	0.3 ± 0.02 (10)*	70.2 ± 1.6 (6)	87.6 ± 1.6 (5)*
<i>Panulirus argus</i>	Marine lobster	Spiny lobster	90.6 ± 2.5 (10)	353.5 ± 7.3 (11)*	306.3 ± 11.4 (4)	498.8 ± 26.8 (3)*
<i>Homarus americanus</i> [#]	Marine lobster	American lobster	124.9 ± 1.2 (20)	624.4 ± 2.8 (20)*	316.0 ± 10.8 (3)	670.0 ± 25.5 (5)*
<i>Procambarus clarkii</i>	Freshwater crayfish	Crayfish	14.5 ± 0.1 (10)	25.9 ± 0.4 (11)*	223.7 ± 6.9 (4)	379.2 ± 8.7 (5)*
<i>Callinectes sapidus</i>	Marine crab	Blue crab	44.9 ± 1.6 (10)	148.4 ± 1.9 (10)*	133.3 ± 1.9 (5)	620.3 ± 17.9 (4)*
<i>Menippe mercenaria</i>	Marine crab	Stone crab	62.7 ± 3.2 (10)	452.5 ± 13.3 (10)*	373.2 ± 23.0 (4)	763.2 ± 33.3 (3)*
<i>Fundulus majalis</i>	Marine teleost	Striped killifish	4.7 ± 0.2 (10)	17.4 ± 0.6 (9)*	64.9 ± 1.6 (5)	119.6 ± 1.6 (6)*
<i>Centropomistis striata</i>	Marine teleost	Black seabass	56.1 ± 1.1 (11)	686.8 ± 7.7 (10)*	85.8 ± 9.0 (4)	208.3 ± 36.8 (3)*
<i>Orthopristis chrysoptera</i>	Marine teleost	Pigfish	7.4 ± 0.4 (10)	91.9 ± 2.9 (10)*	46.1 ± 0.9 (5)	89.9 ± 1.8 (4)*
<i>Lagodon rhomboides</i>	Marine teleost	Pinfish	8.9 ± 0.2 (13)	65.5 ± 2.9 (12)*	57.9 ± 0.8 (6)	81.8 ± 1.4 (5)*
<i>Menicirrhus littoralis</i>	Marine teleost	Gulf kingfish	7.3 ± 0.4 (12)	31.5 ± 0.9 (14)*	45.9 ± 1.4 (5)	72.0 ± 1.4 (9)*
<i>Trachinotus carolinus</i>	Marine teleost	Florida pompano	3.6 ± 0.1 (10)	40.2 ± 1.8 (11)*	46.6 ± 1.3 (3)	78.0 ± 2.2 (6)*
<i>Paralichthys lethostigma</i>	Marine teleost	Southern flounder	26.5 ± 2.2 (12)	530.7 ± 13.8 (12)*	70.1 ± 1.6 (5)	167.7 ± 7.4 (5)*
<i>Lepomis microlophus</i>	Freshwater teleost	Redear sunfish	23.3 ± 2.4 (10)	283.7 ± 6.5 (9)*	79.2 ± 1.6 (6)	102.4 ± 1.5 (7)*
<i>Gymnura micrura</i>	Elasmobranch	Butterfly ray	216.9 ± 5.1 (10)	589.6 ± 21.5 (10)*	79.6 ± 0.8 (4)	116.3 ± 1.3 (5)*

For both body mass and fiber diameter, Kruskal-Wallis analyses found a significant effect of species (†) and

Wilcoxon tests found an effect of size class when all species were pooled (§).

The * indicates a significant difference between size classes within a species (Wilcoxon test).

Values are means ± SEM and N values are in parentheses and represent number of animals (approximately 100 fibers were measured per species and size class to attain mean fiber diameter).

[#]Data for *H. americanus* are from 18.

Table 2

PCr or AP depletion rates and Na⁺-K⁺-ATPase cost and maximal activity. Absolute cost is the difference in rates between treatments ((CN+IA) – (CN+IA+OU)), and fractional cost is absolute cost divided by the rate with CN+IA.

Species	PCr or AP depletion rate (mM min ⁻¹) (CN + IA)		PCr or AP depletion rate (mM min ⁻¹) (CN + IA + OU)		Na ⁺ -K ⁺ -ATPase cost (mM min ⁻¹)		Na ⁺ -K ⁺ -ATPase fractional cost		Na ⁺ -K ⁺ -ATPase activity (μmol min ⁻¹ g ⁻¹)	
	Small [‡]	Large [‡]	Small [‡]	Large [‡]	Small [§]	Large [§]	Small [§]	Large [§]	Small [§]	Large [§]
<i>F. aztecus</i>	0.14 ± 0.01 (5)	0.11 ± 0.01 (5)	0.04 ± 0.02 (5)	0.07 ± 0.01 (8)	0.096	0.046	0.68	0.41	18.96 ± 2.58 (11)	8.83 ± 3.70 (9)*
<i>P. pugio</i>	0.18 ± 0.03 (5)	0.20 ± 0.02 (5)	0.06 ± 0.02 (5)	0.14 ± 0.04 (5)	0.115	0.059	0.64	0.3	31.37 ± 4.16 (13)	29.56 ± 3.86 (11)
<i>P. argus</i>	0.15 ± 0.01 (5)	0.09 ± 0.02 (6)	0.06 ± 0.01 (5)	0.06 ± 0.01 (5)	0.086	0.038	0.57	0.41	15.05 ± 2.81 (10)	11.51 ± 2.18 (11)
<i>H. americanus</i> [#]	0.14 ± 0.01 (5)	0.09 ± 0.18 (5)	0.07 ± 0.01 (5)	0.06 ± 0.01 (5)	0.073	0.036	0.52	0.39	24.03 ± 0.10 (11)	12.80 ± 0.22 (13)*
<i>P. clarkii</i>	0.21 ± 0.02 (5)	0.35 ± 0.02 (6)	0.10 ± 0.02 (5)	0.18 ± 0.02 (5)	0.105	0.171	0.51	0.49	25.96 ± 2.89 (10)	10.94 ± 1.22 (11)*
<i>C. sapidus</i>	0.18 ± 0.26 (5)	0.33 ± 0.04 (5)	0.09 ± 0.02 (5)	0.13 ± 0.01 (5)	0.097	0.199	0.53	0.6	17.26 ± 3.17 (11)	12.90 ± 3.01 (13)
<i>M. mercenaria</i>	0.16 ± 0.02 (5)	0.17 ± 0.02 (5)	0.08 ± 0.02 (5)	0.08 ± 0.01 (5)	0.078	0.092	0.5	0.55	19.81 ± 5.45 (8)	4.16 ± 0.79 (10)*
<i>F. majalis</i>	0.12 ± 0.01 (5)	0.10 ± 0.02 (4)	0.06 ± 0.01 (5)	0.09 ± 0.02 (5)	0.058	0.018	0.49	0.17	7.91 ± 2.23 (10)	5.55 ± 1.26 (9)
<i>C. striata</i>	0.10 ± 0.01 (5)	0.07 ± 0.01 (5)	0.06 ± 0.01 (6)	0.06 ± 0.01 (5)	0.039	0.01	0.38	0.15	3.93 ± 0.43 (15)	3.37 ± 0.61 (17)
<i>O. chrysoptera</i>	0.12 ± 0.01 (5)	0.11 ± 0.02 (4)	0.07 ± 0.01 (5)	0.08 ± 0.01 (6)	0.054	0.035	0.44	0.3	5.92 ± 0.95 (9)	3.97 ± 0.86 (6)
<i>L. rhomboides</i>	0.10 ± 0.03 (5)	0.11 ± 0.01 (6)	0.05 ± 0.01 (8)	0.10 ± 0.01 (6)	0.047	0.008	0.48	0.07	3.09 ± 0.51 (15)	2.77 ± 0.70 (9)
<i>M. littoralis</i>	0.13 ± 0.02 (6)	0.10 ± 0.01 (7)	0.11 ± 0.01 (6)	0.09 ± 0.01 (7)	0.016	0.002	0.13	0.02	11.04 ± 2.82 (11)	3.91 ± 0.71 (13)
<i>T. carolinus</i>	0.13 ± 0.04 (5)	0.09 ± 0.03 (5)	0.09 ± 0.01 (5)	0.08 ± 0.02 (6)	0.04	0.017	0.32	0.18	11.00 ± 1.96 (13)	8.16 ± 1.10 (11)
<i>P. lethostigma</i>	0.11 ± 0.02 (5)	0.10 ± 0.01 (5)	0.08 ± 0.02 (7)	0.09 ± 0.01 (7)	0.033	0.012	0.29	0.13	20.68 ± 3.39 (17)	5.10 ± 0.63 (14)*
<i>L. microlophus</i>	0.07 ± 0.01 (5)	0.08 ± 0.01 (4)	0.05 ± 0.01 (5)	0.06 ± 0.02 (4)	0.016	0.013	0.24	0.17	3.80 ± 0.60 (9)	2.35 ± 0.53 (10)
<i>G. micrura</i>	0.11 ± 0.02 (6)	0.10 ± 0.015 (6)	0.07 ± 0.01 (4)	0.09 ± 0.01 (4)	0.04	0.014	0.36	0.14	3.23 ± 0.79 (10)	2.60 ± 0.44 (10)

Kruskal-Wallis tests found effects of species (†) and

Wilcoxon tests found a difference between inhibitor treatments when all species were pooled (‡) in PCr/AP depletion rate for both size classes.

Absolute and fractional Na⁺-K⁺-ATPase cost was significantly lower in the large size class than the small when all species were pooled (§, Wilcoxon test).

Na⁺-K⁺-ATPase activity had effects of species (†) and

a difference between size classes when species were pooled (§) and

the * indicates significant differences between size classes within a species (Wilcoxon tests).

Values are means ± SEM and N values are in parentheses.

#Data for *H. americanus* are from¹⁸.

Author Manuscript

Author Manuscript

Author Manuscript

Author Manuscript